

Proceedings of the Fifth Annual LHCP
ATL-PHYS-PROC-2017-210
March 13, 2022

Top-quark mass and top-quark pole mass measurements with the ATLAS detector

TERESA BARILLARI

*On behalf of the ATLAS Collaboration
Max-Planck-Institute für Physik
Föhringer Ring 6, 80805 Muenchen, Germany*

ABSTRACT

Results of top-quark mass measurements in the di-lepton and the all-jets top-antitop decay channels with the ATLAS detector are presented. The measurements are obtained using proton-proton collisions at a centre-of-mass energy $\sqrt{s} = 8$ TeV at the CERN Large Hadron Collider. The data set used corresponds to an integrated luminosity of 20.2 fb^{-1} . The top-quark mass in the di-lepton channel is measured to be 172.99 ± 0.41 (stat.) ± 0.74 (syst.) GeV. In the all-jets analysis the top-quark mass is measured to be 173.72 ± 0.55 (stat.) ± 1.01 (syst.) GeV. In addition, the top-quark pole mass is determined from inclusive cross-section measurements in the top-antitop di-lepton decay channel with the ATLAS detector. The measurements are obtained using data at $\sqrt{s} = 7$ TeV and $\sqrt{s} = 8$ TeV corresponding to an integrated luminosity of 4.6 fb^{-1} and 20.2 fb^{-1} respectively. The top-quark pole mass is measured to be $172.9^{+2.5}_{-2.6}$ GeV.

PRESENTED AT

The Fifth Annual Conference
on Large Hadron Collider Physics
Shanghai Jiao Tong University, Shanghai, China
May 15-20, 2017

1 Introduction

Due to the higher centre-of-mass energy, top quark production at the proton–proton (pp) Large Hadron Collider (LHC) is an order of magnitude larger than at the Tevatron. The large data sets of top–antitop quark pairs ($t\bar{t}$) that will be collected at LHC, will allow many precision studies. The top-quark mass, m_{top} , is a fundamental parameter of the Standard Model (SM) and its precise value is indispensable for predictions of cross sections at the LHC. After the Higgs boson discovery at the LHC [1, 2] and in the current absence of direct evidence for new physics beyond the SM, precision theory predictions confronted with precision measurements are becoming an important area of research for self-consistency tests of the SM and in searching for new physics phenomena [3, 4, 5]. Due to the high mass the top-quark’s width is so large that it typically decays before it hadronizes. The m_{top} measurements proceed then via kinematic reconstruction of the top-quark’s decay products, a W boson and a b -quark jet, and comparisons to Monte Carlo (MC) simulations are done. These m_{top} measurements are often referred to as MC top-quark mass, $m_{\text{top}}^{\text{MC}}$, measurements. There is no immediate interpretation of the measured $m_{\text{top}}^{\text{MC}}$ in terms of a parameter of the SM Lagrangian in a specific renormalisation scheme. In many Quantum Chromodynamics (QCD) calculations the top quark pole mass $m_{\text{top}}^{\text{pole}}$, corresponding to the definition of the mass of a free particle, is used as the conventional scheme choice. Present studies estimate that the value of $m_{\text{top}}^{\text{MC}}$ differs from the $m_{\text{top}}^{\text{pole}}$ by $\mathcal{O}(1 \text{ GeV})$ [6, 7]. The $m_{\text{top}}^{\text{pole}}$ can be measured from inclusive $t\bar{t}$ production cross section ($\sigma_{t\bar{t}}$) [8]. However, this $m_{\text{top}}^{\text{pole}}$ determination is currently less precise than the achieved $m_{\text{top}}^{\text{MC}}$ measurements. This is due to the weak sensitivity of the inclusive $\sigma_{t\bar{t}}$ to the $m_{\text{top}}^{\text{pole}}$, but also to the large uncertainties on the factorisation and renormalisation scales, the strong coupling constant α_s , and the proton parton distribution function (PDF). In the following the latest results on the $m_{\text{top}}^{\text{MC}}$, or just m_{top} , measurements in the di-lepton and in the all-jets $t\bar{t}$ decay channel with the ATLAS detector [9] using data at $\sqrt{s} = 8 \text{ TeV}$ are presented. The data set corresponds to an integrated luminosity of 20.2 fb^{-1} . The m_{top} measurements in di-leptonic $t\bar{t}$ decay channel, where each of the top quarks decays into a b -quark, a charged lepton and its neutrino, is further described in Section 2. The m_{top} measurement in the all-jets decay channel involves six jets, two originating from b -quarks and four originating from the two W boson hadronic decays. This recent measurement is detailed in Section 3. Finally, the $m_{\text{top}}^{\text{pole}}$ value is determined from inclusive $\sigma_{t\bar{t}}$ measurements in the di-lepton $t\bar{t}$ decay channel. This analysis uses data collected at $\sqrt{s} = 7 \text{ TeV}$ and 8 TeV and corresponding to an integrated luminosity of 4.6 fb^{-1} and 20.2 fb^{-1} . The achieved $m_{\text{top}}^{\text{pole}}$ results are summarised in Section 4.

2 Di-lepton m_{top} measurements at $\sqrt{s} = 8 \text{ GeV}$

A new measurement of m_{top} is obtained in the $t\bar{t} \rightarrow$ di-lepton decay channel using 2012 data taken at a centre of mass energy $\sqrt{s} = 8 \text{ TeV}$ [10]. The analysis exploits the decay $t\bar{t} \rightarrow W^+W^-b\bar{b} \rightarrow \ell^+\ell^-\nu\bar{\nu}b\bar{b}$, where both W bosons decay into a charged lepton and its corresponding neutrino. In the analysis, the $t\bar{t}$ decay channels ee , $e\mu$ and $\mu\mu$ (including $\tau \rightarrow e, \mu$) are combined and referred to as the di-lepton channel. Single-top-quark events with the same lepton final states are included in the signal. Given the larger data sample compared to the m_{top} measured at $\sqrt{s} = 7 \text{ TeV}$ in ATLAS [11], the event selection was optimised to achieve the smallest total uncertainty. The selection from Ref. [11] is applied as a pre-selection. Here events are required to have a signal from the single-electron or single-muon trigger. Exactly two oppositely charged leptons are required. In the same-lepton-flavour channels, ee and $\mu\mu$, a missing transverse momentum, $E_{\text{T}}^{\text{miss}}$, $> 60 \text{ GeV}$ is required. In addition, the invariant mass of the lepton pair must satisfy $m^{\ell\ell} > 15 \text{ GeV}$, and must not be compatible with the Z mass within 10 GeV . In the $e\mu$ channel the scalar sum of the transverse momentum, p_{T} , of the two selected leptons and all jets is required to be larger than 130 GeV . The presence of at least two central jets with $p_{\text{T}} > 25 \text{ GeV}$ and $|\eta| < 2.5$ is required. Two b -jets taken as originating from the decays of the two top quarks are then selected, and two leptons are taken as the leptons from the leptonic W decays. From the two possible assignments of the two pairs, the combination leading to the lowest average invariant mass of the two lepton- b -jet pairs ($m_{\ell b}^{\text{reco}}$) is retained. Starting from this pre-selection, an optimisation of the total uncertainty in m_{top} is performed. A phase-space restriction based on the average p_{T} of the two lepton- b -jet pairs ($p_{\text{T}\ell b}$) is used to obtain the smallest total uncertainty in

m_{top} , this corresponds to a cut on $p_{T\ell b} > 120$ GeV. To perform the template parameterisation described in Ref. [11], an additional selection criterion is applied. The reconstructed $m_{\ell b}^{\text{reco}}$ value is restricted to the range $30 \text{ GeV} < m_{\ell b}^{\text{reco}} < 170 \text{ GeV}$. Using this selection the kinematic distributions in the data are well described by the predictions. The resulting template fit function based on simulated distributions of $m_{\ell b}^{\text{reco}}$ has m_{top} as the only free parameter and an unbinned likelihood maximisation gives the m_{top} value that best describes the data. Figure 1, left plot, shows the distribution obtained with data together with the fitted probability density functions for the background alone that is hardly visible at the bottom of the figure. The plot on the right side of Figure 1 shows the final corresponding logarithm of the performed likelihood as a function m_{top} . This measurement gives $m_{\text{top}} = 172.99 \pm 0.41$ (stat.) ± 0.72 (syst.) GeV, with the biggest systematic

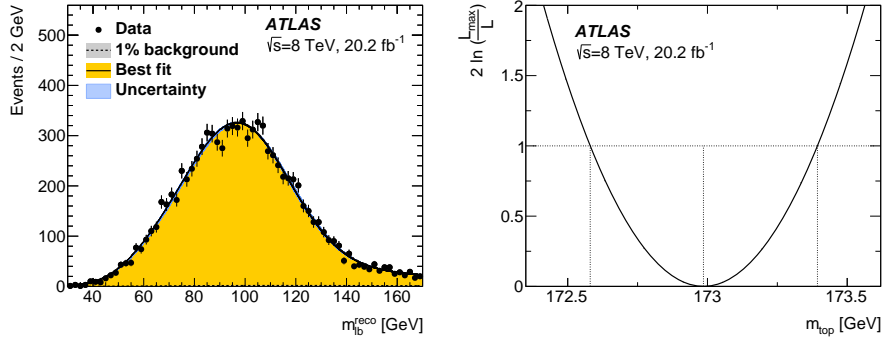


Figure 1: The left plot shows the distribution for data with statistical uncertainties together with the fitted probability density functions for the background alone (barely visible at the bottom of the figure) and for the sum of signal and background. The uncertainty band (invisible) corresponds to the total uncertainty in m_{top} . The corresponding logarithm of the likelihood as a function of m_{top} is displayed in the plot on the right side [10].

uncertainties coming from jet energy scale (JES) and relative b -to-light-jet energy scale. This m_{top} result is $\sim 40\%$ more precise than m_{top} measured at $\sqrt{s} = 7$ TeV. It is the most precise single result in this decay channel to date. A combination with the ATLAS measurements in the $t\bar{t} \rightarrow \text{lepton} + \text{jets}$ and $t\bar{t} \rightarrow \text{di-lepton}$ decay channels from $\sqrt{s} = 7$ TeV data is performed. Using a dedicated mapping of uncertainty categories, the combination of the three measurements results in a value of $m_{\text{top}} = 172.84 \pm 0.34$ (stat.) 0.61 (syst.) GeV. This result is mostly limited by the calibration of the JES and by the Monte Carlo modeling of signal events.

3 All-jet m_{top} measurements at $\sqrt{s} = 8$ GeV

A recent m_{top} measurement obtained using ATLAS data taken at $\sqrt{s} = 8$ TeV [12] exploits the decay $t\bar{t} \rightarrow W^+ b W^- \bar{b} \rightarrow q\bar{q}' b q'' \bar{q}''' \bar{b}$, where both W bosons decay into jets from charged quarks, q . This is a challenging measurement to make because of the large multi-jet background arising from various other processes of the strong interaction described by the QCD. However, all-jets $t\bar{t}$ events profit from having no neutrinos among the decay products, so that all four-momenta can be measured directly. The multi-jet background for the all-hadronic $t\bar{t}$ channel, while large, leads to different systematic uncertainties than in the case of the single- and di-leptonic $t\bar{t}$ channels. Thus, all-jets analyses offer an opportunity to cross-check m_{top} measurements performed in the other channels. Events in this analysis are selected by a trigger that requires at least five jets with $p_T > 55$ GeV. Events with isolated electrons (muons) with $E_T > 25$ GeV ($p_T > 20$ GeV) and reconstructed in the central region of the detector (within $|\eta| < 2.5$) are rejected. To ensure that the selected events are in the plateau region of the trigger efficiency curve where the trigger efficiency in data is greater than 90%, at least five of the reconstructed central jets are required to have $p_T > 60$ GeV. Any additional central jet is required to have $p_T > 25$ GeV. Events containing neutrinos are removed by requiring $E_T^{\text{miss}} < 60$ GeV. In the final selection, events are kept if at least two of the six leading transverse momentum jets are identified as originating from a b -quark ($N_{b\text{tag}}$). Such jets are said to be b -tagged. In each event the

two jets with leading b -tag weights (b_i and b_j) are required to be within an azimuthal angle $\Delta\phi(b_i, b_j) > 1.5$. Finally, another cut based on the azimuthal angle between b -jets and their associated W boson candidate is applied: the average of the two angular separations for each event is required to satisfy $\langle\Delta\phi(b, W)\rangle < 2$. To determine the m_{top} in each $t\bar{t}$ event, a minimum- χ^2 approach is adopted where all possible permutations of the six or more reconstructed jets in each event are considered. The permutation resulting in the lowest χ^2 value is kept. To reduce the multi-jet background in the analysis and to eliminate events where the top quarks and the W bosons in an event are not reconstructed correctly, a $\chi^2 < 11$ is required. The dominant multi-jet background in the analysis is determined directly from the data. Two uncorrelated variables, the $N_{b_{\text{tag}}}$ and the $\langle\Delta\phi(b, W)\rangle$, are used to divide the data events into four different regions, such that the background is determined in the control regions and extrapolated to the signal region. The four regions are labeled ABCD and distributions of the ratio of three-jet to dijet masses ($R_{3/2} = m_{jjj}/m_{jj}$) are studied for each of the defined regions. The $R_{3/2}$ observable is chosen due to its reduced dependence on the JES uncertainty. To extract a measurement of the m_{top} , a template method with a binned minimum- χ^2 approach is employed. For each $t\bar{t}$ event, two $R_{3/2}$ values are obtained, one for each m_{top} measurement. Signal and background templates binned in $R_{3/2}$ are created using simulated $t\bar{t}$ events, and the data-driven background distribution. After applying a final χ^2 fit, which uses matrix algebra to include non-diagonal covariance matrices, m_{top} is measured to be: $m_{\text{top}} = 173.72 \pm 0.55$ (stat.) ± 1.01 (syst.) GeV. Figure 2 shows the $R_{3/2}$ distribution, left plot, with the corresponding total fit as well as its decomposition into signal and the multi-jet background. The right plot in this figure shows the ellipses corresponding to 1- σ (solid line) and 2- σ (dashed line) variations in statistical uncertainty. The dominant sources of systematic uncertainty

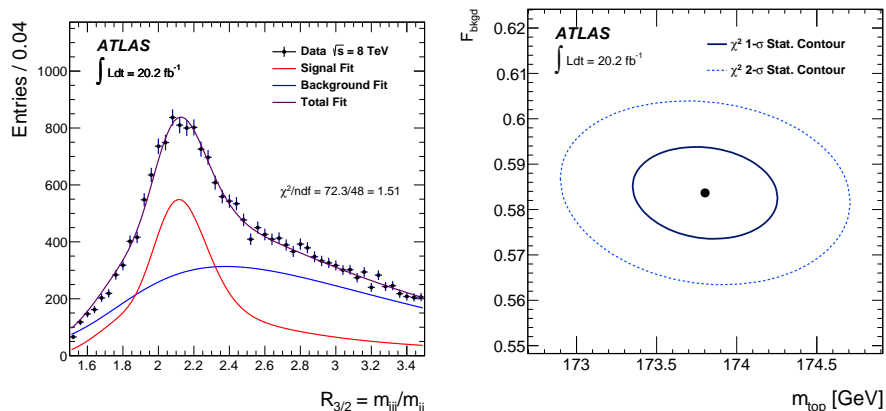


Figure 2: The left plot shows the $R_{3/2}$ distribution in data with the total fit (in magenta) and its decomposition into signal (in red) and the multi-jet background (in blue). The errors shown are statistical only. The right plot shows the ellipses corresponding to the 1- σ (solid line) and 2- σ (dashed line) statistical uncertainty. The central point in the figure indicates the values obtained for m_{top} on the x -axis, and the fitted background fraction, obtained within the fit range of the $R_{3/2}$ distribution on the y -axis. The plots do not take into account the small bias correction described in Ref. [12]. The final top-quark mass is 173.72 ± 0.55 (stat.) ± 1.01 (syst.) GeV.

in this m_{top} measurement, despite the usage of the $R_{3/2}$ observable, come from the JES, hadronisation modelling and the b -jet energy scale. This measurement is about 40% more precise than the previous m_{top} measurement performed by ATLAS in the all-hadronic channel $\sqrt{s} = 7$ TeV [13].

4 Measurement of $m_{\text{top}}^{\text{pole}}$ in di-leptonic events at $\sqrt{s} = 7$ and 8 TeV

At the LHC, precise measurements of $\sigma_{t\bar{t}}$ are sensitive to the uncertainty on α_s , to the gluon parton distribution function (PDF), the m_{top} , and potential enhancements of the cross-section due to physics beyond

the Standard Model. In the following the $m_{\text{top}}^{\text{pole}}$ determination from the inclusive $\sigma_{t\bar{t}}$ measurement in the di-leptonic $e\mu$ channel, $t\bar{t} \rightarrow W^+Wb\bar{b} \rightarrow e^\pm\mu^\pm\nu\bar{\nu}b\bar{b}$, is presented [14]. The main background comes from the associated production of a W boson and a single top quark, the so called Wt single top background. The analysis is performed on the ATLAS 2011 - 2012 pp collision data sample, corresponding to integrated luminosities of 4.6fb^{-1} at $\sqrt{s} = 7\text{TeV}$ and 20.3fb^{-1} at $\sqrt{s} = 8\text{TeV}$. Events were required to pass either a single-electron or single-muon trigger, with thresholds chosen such that the efficiency plateau is reached for leptons with $p_T > 25\text{GeV}$. MC simulated event samples were used to develop the analysis, to compare to the data and to evaluate signal and background efficiencies and uncertainties. The analysis makes use of reconstructed electrons, muons and b -tagged jets. A preselection requiring exactly one electron and one muon was applied. Events with an opposite sign $e\mu$ pair constituted the main analysis sample, whilst events with a same-sign $e\mu$ pair were used in the estimation of the background from misidentified leptons. The production cross-section $\sigma_{t\bar{t}}$ was determined by counting the numbers of opposite-sign $e\mu$ events with exactly one and exactly two b -tagged jets and was measured to be $\sigma_{t\bar{t}} = 182.9 \pm 3.1 \pm 4.2 \pm 3.6 \pm 3.3\text{pb}$ at $\sqrt{s} = 7\text{TeV}$, and $\sigma_{t\bar{t}} = 242.4 \pm 1.7 \pm 5.5 \pm 7.5 \pm 4.2\text{pb}$ at $\sqrt{s} = 8\text{TeV}$. where the four uncertainties arise from data statistics, experimental and theoretical systematic effects related to the analysis, knowledge of the integrated luminosity and of the LHC beam energy. The strong dependence of the theoretical prediction for $\sigma_{t\bar{t}}$ on m_{top} , offers the possibility of interpreting measurements of $\sigma_{t\bar{t}}$ as measurements of m_{top} . The theoretical calculations use $m_{\text{top}}^{\text{pole}}$ for predictions. The dependence of the cross-section predictions on $m_{\text{top}}^{\text{pole}}$ is shown in Figure 3, left plot, at $\sqrt{s} = 7$ and 8TeV . The function proposed in Ref. [15] was used to parameterise the dependence

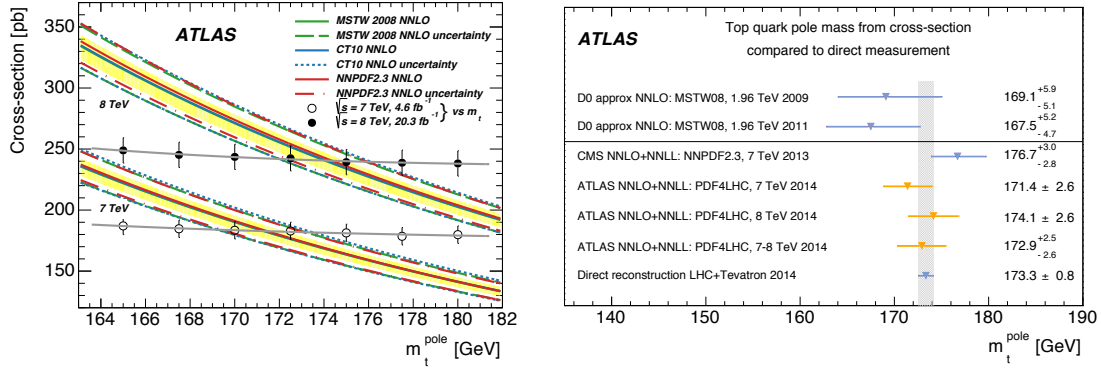


Figure 3: Left plot shows predicted NNLO+NNLL production $\sigma_{t\bar{t}}$ at $\sqrt{s} = 7\text{TeV}$ and $\sqrt{s} = 8\text{TeV}$ as a function of $m_{\text{top}}^{\text{pole}}$ showing the central values (solid lines) and total uncertainties (dashed lines) with several PDF sets. The yellow band shows the QCD scale uncertainty. The measurements of $\sigma_{t\bar{t}}$ are also shown. The right plot shows comparison of $m_{\text{top}}^{\text{pole}}$ values determined from this and previous $\sigma_{t\bar{t}}$ measurements [16, 17], also shown is the m_{top} from direct measurements obtained from the LHC+Tevatron combinations [18].

of $\sigma_{t\bar{t}}$ on m_{top} separately for each of the NNLO PDF sets CT10 [19, 20], MSTW [21] and NNPDF2.3 [22], together with their uncertainty. The left plot in Figure 3 also shows the small dependence of the experimental measurement of $\sigma_{t\bar{t}}$ on the assumed value of m_{top} , arising from variations in the acceptance and Wt single top background. A comparison of the theoretical and experimental curves shown in this plot allows an unambiguous extraction of $m_{\text{top}}^{\text{pole}}$. The extraction is performed by maximising using a Bayesian likelihood as a function of $m_{\text{top}}^{\text{pole}}$ [14]. The likelihood fit maximised separately for each PDF set and centre-of-mass energy to give $m_{\text{top}}^{\text{pole}}$ values shown in Table 1. A single $m_{\text{top}}^{\text{pole}}$ value was derived for each centre-of-mass energy giving $m_{\text{top}}^{\text{pole}} = 171.4 \pm 2.6\text{GeV}$ ($\sqrt{s} = 7\text{TeV}$) and $m_{\text{top}}^{\text{pole}} = 174.1 \pm 2.6\text{GeV}$ ($\sqrt{s} = 8\text{TeV}$). Considering only uncorrelated experimental uncertainties, the two values are consistent at the level of 1.7 standard deviations. Finally, $m_{\text{top}}^{\text{pole}}$ was extracted from the combined $\sqrt{s} = 7\text{TeV}$ and $\sqrt{s} = 8\text{TeV}$ dataset using the product of likelihoods for each centre-of-mass energy and accounting for correlations via nuisance parameters. The resulting value using the envelope of all three considered PDF sets is $m_{\text{top}}^{\text{pole}} = 172.9^{+2.5}_{-2.6}\text{GeV}$. All extracted

PDF	$m_{\text{top}}^{\text{pole}}$ GeV from $\sigma_{t\bar{t}}$	
	$\sqrt{s} = 7 \text{ TeV}$	$\sqrt{s} = 8 \text{ TeV}$
CT10 NNLO [19, 20]	171.4 ± 2.6	171.1 ± 2.6
MSTW 68% NNLO [21]	171.2 ± 2.4	174.0 ± 2.5
NNPDF2.3 5f FFN [22]	$171.3^{+2.2}_{-2.3}$	174.2 ± 2.4

Table 1: Measurements of the $m_{\text{top}}^{\text{pole}}$ determined from the $t\bar{t}$ cross-section measurements at $\sqrt{s} = 7 \text{ TeV}$ and $\sqrt{s} = 8 \text{ TeV}$ using various PDF sets.

values are consistent with the m_{top} or $m_{\text{top}}^{\text{MC}}$ measurements obtained from kinematic reconstruction of $t\bar{t}$ events, see right plot in Figure 3.

References

- [1] ATLAS Collaboration, Phys. Lett. B **716**, 1 (2012) [arXiv:1207.7214 [hep-ex]].
- [2] CMS Collaboration, Phys. Lett. B **716**, 30 (2012) [arXiv:1207.7235 [hep-ex]].
- [3] G. Degrossi *et al.*, JHEP **08**, 098 (2012) [arXiv:1205.6497 [hep-ph]].
- [4] M. Baak *et al.* [Gfitter Group], Eur. Phys. J C **9**, 74 (2014) [arXiv:1407.3792 [hep-ph]].
- [5] S. Alekhin *et al.*, Phys. Lett. **B716**, 214-219 (2012) [arXiv:1207.0980 [hep-ph]].
- [6] S. Moch *et al.*, DESY-14-081, (2014) [arXiv:1405.4781 [hep-ph]].
- [7] S. Moch, DESY-14-147, (2014) [arXiv:1408.6080 [hep-ph]].
- [8] U. Langenfeld *et al.*, Phys. Rev. **D80** (2009) [arXiv:0906.5273 [hep-ph]].
- [9] ATLAS Collaboration, JINST **3** S08003 (2008) [arXiv:1702.07546 [hep-ex]].
- [10] ATLAS Collaboration, Phys. Lett. **C75** (2016) [arXiv:1606.02179 [hep-ex]].
- [11] ATLAS Collaboration, Eur. Phys. J. **C75** (2015) [arXiv:1503.05427 [hep-ex]].
- [12] ATLAS Collaboration, JHEP 09 **118** (2017) [arXiv:1702.07546 [hep-ex]].
- [13] ATLAS Collaboration, Eur. Phys. J. **C75** (2015) [arXiv:1409.0832 [hep-ex]].
- [14] ATLAS Collaboration, Eur. Phys. J. **C74** (2014) [arXiv:1406.5375 [hep-ex]].
- [15] M. Czakon, P. Fiedler, and A. Mitov, Phys. Rev. Lett. **110** (2013) [arXiv:1303.6254 [hep-ph]].
- [16] V. Abazov *et al.* [D0], Phys. Lett. **B703** (2011) [arXiv:1104.2887 [hep-ex]].
- [17] CMS Collaboration, Phys. Lett. **B728** (2014) [arXiv:1307.1907 [hep-ex]].
- [18] [ATLAS, CDF, CMS, D0], [arXiv:1403.4427 [hep-ex]].
- [19] H. L. Lai *et al.*, Phys. Rev. **D82** (2010) [arXiv:1007.2241 [hep-ph]].
- [20] J. Gao *et al.*, Phys. Rev. **D89** (2014) [arXiv:1302.6246 [hep-ph]].
- [21] A. D. Martin *et al.* Eur. Phys. J. **C63** (2009) [arXiv:0901.0002 [hep-ph]].
- [22] R. Ball *et al.*, Nucl. Phys. **B867** (2013) [arXiv:1207.1303 [hep-ph]].